a Quasi-Steady MPD Accelerator," Ph.D. thesis, Aerospace and Mechanical Sciences Rept. 1041, May 1972, Princeton University, Princeton, N.J.

[12] Bohn, W. L. et al., "On Spectroscopic Measurements of Velocity Profiles and Non-Equilibrium Radial Temperatures in an Argon Plasma Jet," *Journal of Quantitive Spectroscopy and Radiative Transfer*, Vol. 7, 1967, pp. 661–676.

[13] Clark, K. E. et al., "Quasi-Steady Magnetoplasmadynamic Arc Characteristics," AIAA Paper 70-1095, Stanford, Calif., 1970.

[14] Jahn, R. G. et al., "Pulsed Electromagnetic Gas Acceleration," NASA NGL 31-001-005, Aerospace and Mechanical Sciences Rept. 634q, July 1971, Princeton University, Princeton, N.J.

[15] Bruckner, A. P. and Jahn, R. G., "Exhaust Plume Structure in a Quasi-Steady MPD Arc," AIAA Paper 72-499, Bethesda, Md., 1972.

[16] Jahn, R. G. et al., "Pulsed Electromagnetic Gas Acceleration," NASA NGL 31-001-005, Aerospace and Mechanical Sciences Rept. 634s, July 1972, Princeton University, Princeton, N.J.

[17] Jahn, R. G. et al., "Pulsed Electromagnetic Gas Acceleration," NASA NGL 31-001-005, Aerospace and Mechanical Sciences Rept. 634t, Jan. 1973, Princeton University, Princeton, N.J.

[18] Meissner, K. W., "Interference Spectroscopy," *Journal of the Optical Society of America*, Vol. 31, No. 6, June 1941, pp. 405–427.

[19] Jacquinot, P., "New Developments in Interference Spectroscopy," *Reports on Progress in Physics*, Vol. XXII, 1960, pp. 267–312.

[20] Greig, J. R. and Cooper, J., "Rapid Scanning with the Fabry-Perot Etalon," *Applied Optics*, Vol. 7, No. 11, Nov. 1968, pp. 2166–2170.

[21] Jahn, R. G. et al., "Pulsed Electromagnetic Gas Acceleration," NGL 31-001-005, Aerospace and Mechanical Sciences Rept. 634r, Jan. 1972, Princeton University, Princeton, N.J.

[22] von Jaskowsky, W. F., private communication, 1973, Dept. of Aerospace and Mechanical Sciences, Princeton University, Princeton, N.J.

[23] Zel'dovich, Ya. B. and Raizer, Yu. P., *Physics of Shock Waves and High Temperature Hydrodynamic Phenomena*, Academic Press, New York, 1966, Vol. 1, pp. 406–413 and Vol. 2, pp. 571–585.

AIAA JOURNAL VOL. 12, NO. 9

Jet-Diagnostics of a Self-Field Accelerator with Langmuir Probes

F. MAISENHÄLDER* AND W. MAYERHOFER†
DFVLR-Institut für Plasmadynamik, Stuttgart, F. R., Germany

Cylindrical electric probes of the Langmuir type are used to investigate the jet of a self-field plasma accelerator. The test conditions with argon as propellant range from $I = 2000$ amp to 4500 amp and $\dot{m} = 0.3$ g/sec to 1.0 g/sec. The pattern of the flow direction, the radial and axial distributions of the electron temperature, the ion density, the static pressure, the ratio of directed to thermal velocity, and the ion velocity are determined. The electron temperature profiles show steep gradients from the axis of the jet to a radius of about 8 cm. Beyond this radius the temperatures remain at a nearly constant value of $8-10\times10^3$K in the whole visible region of the jet with a diameter of about 1 m. The influence of the angle of attack on the determination of the electron temperature turns out to be not severe. The ion densities, calculated from the ion saturation currents and the electron temperatures, are affected by the discharge currents and the mass flow rates. In the axis peak values are observed up to 5×10^{14} cm^{-3}. An increase of the mass flow rate causes large radial density gradients over a wide range of the diameter. The calculated distributions of the static pressure show that "entrainment" can be excluded. This is confirmed by the flow pattern of the ions and the total gas too. The ratios of V/V_{th} (a quantity which may be regarded as a Mach number) are in good agreement with calculated Mach numbers. The profiles of the ion velocity show a reasonable behavior. The mass flow through a cross section of the jet calculated from the velocity and density profiles is in good agreement with the applied mass flow rate. Observations of characteristic parameters show that in a wide region of the plasma the probes are operated collision free, but that in the axis near the nozzle exit a transition regime to collision-dominated conditions is present.

Introduction

THE plasma accelerator of the self-magnetic or self-field coaxial type may be operated continuously or pulsed. The pulsed quasi-steady version[1–5] probably will find its main application as a thruster. The continuously working accelerator designed for purposes of propulsion too, will have its near future application as a wind-tunnel device. Theoretical and experimental investigations of this accelerator have been done by Hügel.[6,7] For reasons of completeness a short description of the mechanism of this type of accelerator will be given here.

The thruster consists of a cathode made of thoriated tungsten, an arc chamber, and an expansion nozzle. Arc chamber and nozzle are made of individual water-cooled segments which are insulated against each other by layers of alumina (Fig. 1). The propellant is fed along the cathode. The last and largest of the segments represents the anode. The outer surface of the accelerator, with exception of the anode front face, is insulated by a layer of alumina too, thus achieving a well defined onset of the discharge current. Two mechanisms contribute to the plasma acceleration: 1) electrothermal heating of the plasma and expansion in the nozzle, and 2) acting of $\mathbf{j}\times\mathbf{B}$ volume forces

Presented as Paper 73-1095 at the AIAA 10th Electric Propulsion Conference, Lake Tahoe, Nev., October 31–November 2, 1973; submitted November 26, 1973; revision received March 25, 1974. The authors wish to thank Th. Peters who sponsored this work. Furthermore we would like to acknowledge the assistance of F. Albrecht and R. Jacobson in constructing the test facilities and of M. Kling in establishing the programs for the evaluation of the data.

Index categories: Plasma Dynamics and MHD; Electric and Advanced Space Propulsion.

* Senior Research Scientist.

† Research Scientist.

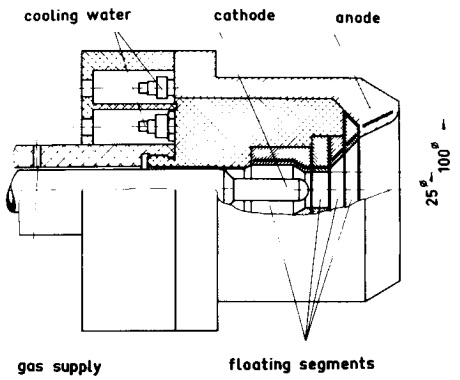

Fig. 1 Schematic view of the thruster.

formed by the discharge current and the azimuthal self-magnetic field. This electromagnetic effect is proportional to I^2 (I, discharge current) and $\ln(r_a/r_c)$ (r_a, radius of anode onset; r_c, radius of cathode onset of the discharge).

In order to investigate the jet of such an apparatus, we used cylindrical Langmuir probes as a diagnostic tool. We determined radial and axial distributions of the electron temperature, the ion density, the direction of ion flow, and a Mach number, based on the most probable thermal velocity. From there other quantities like partial pressure, conductivity, mass flow, magnetic Reynolds number, etc., can be calculated. We used the same operating conditions where thrust, Pitot pressure, and flowing direction of the gas have been measured[7] and furthermore the behavior of discharge stability in dependence of current and mass flow rate has been investigated. With argon as the propellant and an ambient pressure of about 5×10^{-2} torr, combinations of current and mass flow rate have been investigated and are presented in Table 1.

Table 1 Combination of the operating conditions

mass flow rate \ current	2000 amp	2400 amp	3500 amp	4500 amp
0.3 g/sec	x	x		
0.6 g/sec	x		x	
1.0 g/sec	x			x

Most of the figures in this paper refer to the operating conditions

$$I = 2000 \text{ amp}, \quad \dot{m} = 0.3 \text{ g/sec}$$
$$I = 4500 \text{ amp}, \quad \dot{m} = 1.0 \text{ g/sec}$$

It is not the purpose of this paper to explain physical mechanisms and performances of the accelerator in detail; it should be rather taken as a contribution to the diagnostics of the jet of an already well-discussed apparatus.[6,7]

Measurements, Results, and Discussions

The accelerator was mounted in a 2-m-diam, 5-m long stainless-steel vacuum tank. We usually used a double-probe arrangement with the main axis of the one cylindrical probe oriented vertically and of the other horizontally. The probe material was tungsten and the probe wire dimensions were 0.5-mm diam, 20-mm length, and 0.15-mm diam and 10 mm length, respectively. The probe with the larger dimensions was used, when the gasdynamic properties of the jet were such, that the probe was heated up too much and bent off.

The probe wires were guided in capillary tubes made of alumina which themselves were shielded by a copper tube. This shielding tube was insulated from the plasma by a layer of alumina again. The diameter of the whole probe arrangement was about 5 mm. By means of a special apparatus the probes could be moved in radial and axial direction allowing measurements at each point of a horizontal plane through the jet axis. The current vs voltage characteristics were achieved by applying an alternating voltage to the probes with respect to a large electrode (metallic wall of the vacuum tank). Thus in all cases, the probes were operated as single Langmuir probes. The characteristics were recorded by a storage oscilloscope.

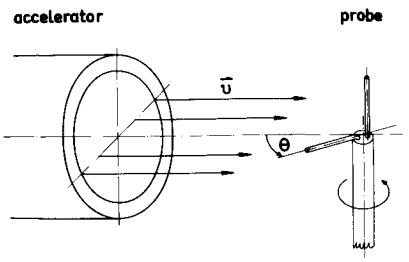

Fig. 2 Schematic view of the probe arrangement.

Flow Direction

It is useful to know the flow direction of the ions in order to draw a flow pattern of the accelerator and, as will be seen in the next section, it is necessary to know it in order to determine the Mach number. From literature[8,9] it is known that the ion saturation current of cylindrical Langmuir probes with a large ratio of length to diameter is a function of the directed ion velocity and of the angle θ, formed by the main axis of the probe and the flow direction.

With flow velocities V much higher than the thermal ion speed $(2KT_i/m_i)^{1/2}$, the ion saturation current depending on the angle should become[8]

$$I_{is} \sim (C_1 + \sin^2\theta)^{1/2}$$

This means that the ion saturation current should become sinusoidal with minima at $\theta = 0°$ and 180°, and maxima at $\theta = 90°$ and 270°.

We used a probe arrangement as shown in Fig. 2, rotated it as indicated and recorded the ion saturation current of the horizontally oriented probe in dependence of the angle θ, where now θ is the deviation from the centerline of the jet. A typical plot of the ion saturation current is shown in Fig. 3. The angles of minimum current indicate the direction of the ion flow. With knowledge of the angles at several points in radial and axial distances it is possible to draw the ion flow pattern of the plasma jet.

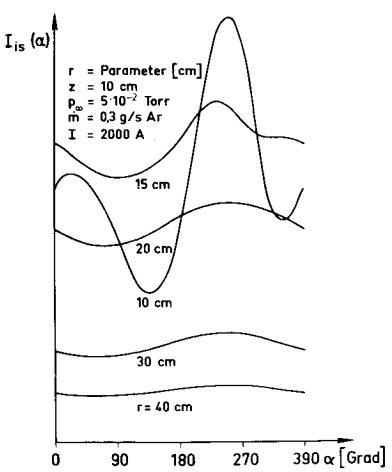

Fig. 3 Angular dependence of the ion saturation current.

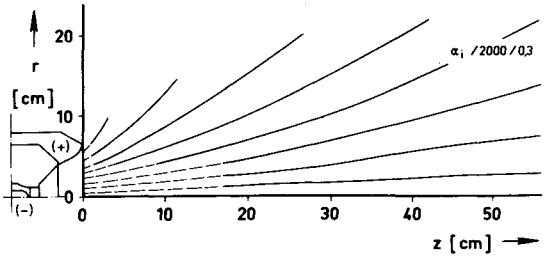

Fig. 4 Flow pattern (ions) at $I = 2000$ amp; $\dot{m} = 0.3$ g/sec.

For the operating conditions $I = 2000$ amp, $\dot{m} = 0.3$ g/sec, and $I = 4500$ amp, $\dot{m} = 1$ g/sec this is shown in Fig. 4 and Fig. 5, respectively. The full lines mark the streamlines, measured in the described manner. In the region of the dashed lines this method was not applicable because of the high heat flux to the probes. This part of a streamline is extrapolated from the measured one. The end of the full lines marks the limit of the method towards larger radial distances and gives a sort of boundary of the jet. This behavior can be explained as follows. Observing Fig. 3, where the angular dependence of the ion saturation current is plotted vs the angle θ, only the curves at $r =$ 10 cm and smaller radii (not drawn in this figure) show the expected behavior. The currents at $r = 20$ cm and at larger radii show only one maximum at about $\theta = 270°$ and one minimum in the neighborhood of $\theta = 90°$, whereas the curve at $r = 15$ cm has an intermediate behavior. Furthermore the position of the extremes is fairly independent of r and z. Observing the plasma parameters with regard to this behavior we found that the transition from one case to the other, represented by the intermediate curve, occurred at values of $V/V_{th} \approx 0.7$. This indicates that the influence of the directed velocity on the collection of ions becomes negligible and the ion saturation current is dominated by the electron temperature and the ion density. Because the effect is proportional to $(T_e)^{1/2}$, the influence of T_e is not strong and in most cases negligible. It can be shown[10] that the gradient of the ion density in a first approximation causes an angular dependence of the ion saturation current according to the equation

$$I_{is} = C_1 + C_2 \sin\theta$$

Here C_1 and C_2 represent constants which may be calculated from the radial distribution of the ion density.

This behavior becomes evident by observing the motion of a small area in the middle of the horizontal probe wire along a circular path through regions of various ion densities. Beginning the movement at $\theta = 0°$ and a medium density to $\theta = 90°$ and a lower density, further to $\theta = 180°$ and again a medium density and $\theta = 270°$ and a high density and returning to the starting point, this motion causes a sinusoidal portion of the ion saturation current.

It is obvious from these considerations that the applied method is limited to a region of the jet, where the directed velocity of the ions is larger than the thermal velocity. Perhaps it is reasonable to define this flow dominated region of the exhaust plasma as the "jet."

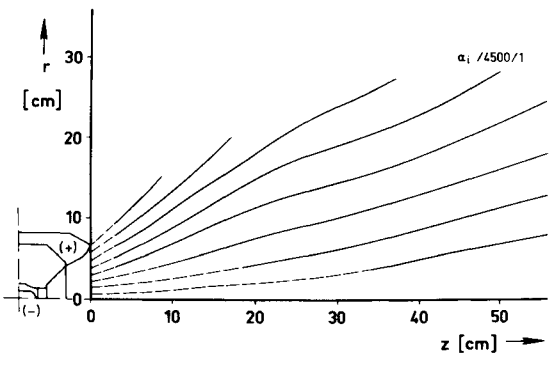

Fig. 5 Flow pattern (ions) at $I = 4500$ amp; $\dot{m} = 1$ g/sec.

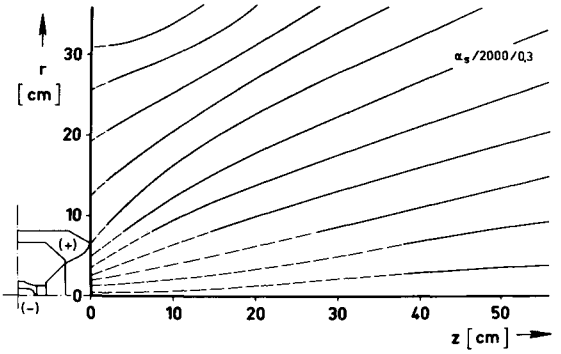

Fig. 6 Flow pattern (gas) at $I = 2000$ amp; $\dot{m} = 0.3$ g/sec.

Above all, it is important to know this angular behavior when measuring the current ratio of cylindrical probes aligned and perpendicular to the flow direction in order to determine the flow velocities of the ions, as will be outlined in the next section.

In order to determine the flow direction beyond the mentioned boundary at larger radial distances, we used a very easily movable mica vane which was brought into the plasma jet. This vane took orientation to the flow direction of the whole gas (neutrals and ions). The streamlines obtained in this manner for a current of 2000 amp and a mass flow rate of 0.3 g/sec are shown in Fig. 6. The mica-vane method is not applicable in regions of high temperature, i.e., in the axis of the jet and near the nozzle exit. In the overlapping region where both methods can be applied, they show very good agreement. This means that the flow direction of the ions is the same as that of the total gas in a wide range of the jet. This is a reasonable result with regard to a very high degree of ionization in the jet which has been observed by spectroscopic investigations. At larger radial position the ion flow seems to have a greater component in radial direction than the whole gas. This behavior can be explained by diffusion of the ions and by $\mathbf{j} \times \mathbf{B}$ forces acting away from the axis as pointed out in Ref. 11. Because in this region the ion densities are low (see next section), this has no remarkable effect upon the integral performance data of the accelerator. It is worthwhile mentioning that there is a very good agreement with measurements of the flow direction done with an aerodynamic yaw probe.[6]

It can be seen from the flow pattern that the plasma jet is more divergent with lower mass flow rates and higher currents. Since in a region far downstream of the nozzle exit the effect of $\mathbf{j} \times \mathbf{B}$ forces is negligible (measurements of the current distribution within the plasma jet indicate that less than 3% of the total current extend farther than 15 cm downstream),[11] this behavior is regarded to be a thermodynamic effect.

Furthermore it can be seen that the mentioned boundary ($V/V_{th} \approx 0.7$), where the method of the angular dependence of the ion saturation current fails, moves to smaller radial distances with increasing mass flow rate. The reason for this may be an increase of V_{th} or a decrease of V. As may be seen later from the electron temperature distributions, T_e is constant and about 10,000 K as a first approximation in this particular region, thus indicating that V_{th} is almost constant (see next section) and hence V must decrease. This is in accordance with the theoretically predicted behavior of V ($V \sim I^2/\dot{m}$), where V decreases with increasing mass flow rate.

Mach Number and Velocities

In the previous section we pointed out that the ion saturation current of cylindrical Langmuir probes is a function of the angle θ and of the directed velocity V of the ions. The angular dependence enabled the construction of the flow pattern. Now we

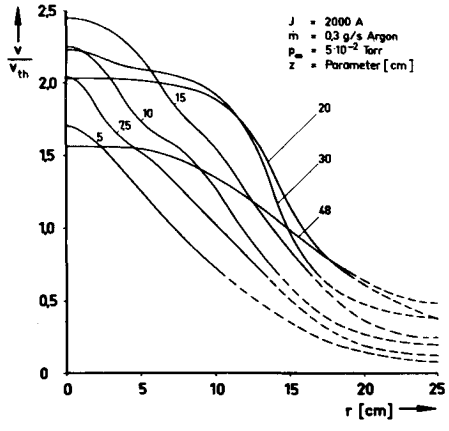

Fig. 7 Radial distributions of the ratio V/V_{th}; $I = 2000$ amp; $\dot{m} = 0.3$ g/sec..

use the influence of the velocity V on the probe current to determine a Mach number.

The basic theoretical treatment of this problem has been done by Kanal.[12] The ratio of the ion saturation currents of two cylindrical Langmuir probes with identical geometrical areas, the one probe aligned and the second perpendicular to the flow direction, is given by the following expression:

$$\frac{I_\perp}{I_\parallel} = \frac{2}{\pi^{1/2}} e^{-(V/V_{th})^2} \sum_{n=0}^{\infty} \left[\frac{(V/V_{th})^n}{n!}\right]^2 \Gamma\left(n+\frac{3}{2}\right)$$

V = velocity of the flowing plasma; V_{th} = most probable thermal speed of the particles, $V_{th} = (2KT_i/m_i)^{1/2}$; and Γ = gamma function.

The measurements are done with the same arrangement as shown in Fig. 2, which is moved at various distances z from the nozzle exit of the accelerator through a diameter. According to the flow pattern we put the horizontally oriented probe outside of the jet in the angular position which corresponds to the flow direction at that point (z,r) where the measurement is intended to be done. Now the probe arrangement is moved through the jet along a diameter and at the chosen point the (normally turned off) writing beam of a storage oscilloscope is turned on during the time of one period of the alternating voltage with which the probes are operated. Thus the current-voltage characteristics of the two single-operated Langmuir probes are stored on the oscilloscope screen. With the aid of a hard copy unit, this screen picture is transferred to paper.

The equation for $I_\perp/I_\parallel$ is based on the assumption of negligible sheath thickness.[13] It is known that the diameter of the sheath between probe and plasma decreases as the probe potential approaches the plasma potential. Calculations and observations while evaluating the curves showed that it is suitable to extrapolate the determined curves of the ion saturation current to the floating potential. The values of $I_\perp$ and $I_\parallel$ obtained in this manner are used to determine V/V_{th}.

With the mentioned operating conditions and the electron temperature distributions of the next section in mind, the gas should be fully ionized in the interacting parts of the jet. Furthermore, spectroscopic measurements[14] showed that the ion temperatures are not very different from the electron temperatures. Hence the most probable thermal speed of the ions is approximately equal to the speed of sound. Therefore the ratio V/V_{th} is in a good approximation equal to the Mach number of the total plasma.

These ratios V/V_{th} as a function of the radial distance from the axis of the jet and for the operating conditions $I = 2000$ amp, $\dot{m} = 0.3$ g/sec; $I = 4500$ amp, $\dot{m} = 1$ g/sec are shown in Figs. 7 and 8. As pointed out in the previous section the ion saturation current in the region $V/V_{th} \gtrsim 0.7$ is dominated rather by the gradients of T_e and n_i than by the flow of the ions; therefore the behavior of V/V_{th} below this boundary is taken to be uncertain and marked by the dashed lines.

Analyzing the curves it can be observed that the smallest profile of the ratio V/V_{th} is in front of the nozzle. The profiles widen in radial direction with increasing distance z from the nozzle exit as it may be expected from a freejet behavior. The peak values of V/V_{th} (in the axis) increase too with the distance z until they reach the maximum at distances of 15 cm at low mass flow rates and of about 30 cm with higher mass flows. Beyond this region the V/V_{th} ratio decreases with a further increase of z. This behavior is similar at all test conditions. The widths of the profiles become smaller with increasing mass flow rates. The highest value $V/V_{th} = 2.85$ is observed 30-cm downstream from the nozzle exit in the axis of a jet with $I = 4500$ amp, $\dot{m} = 1$ g/sec.

It should be mentioned that the values of V/V_{th} are in good agreement with Mach numbers calculated by Hügel based on measured pitot pressures and using data of T_e and n_i presented herein.

Hence it is possible to calculate the radial and axial distributions of the ion velocity. To do this, the distribution of the ion temperature must be known. At the moment we can assume that the ion temperature is proportional to the electron temperature. Because the determination of V/V_{th} tends to yield too small values because of the angular dependence of the ion saturation current, the ion temperature is assumed to be equal to the electron temperature ($T_i = T_e$), an assumption confirmed by first results of spectroscopic measurements.[14] Thus the shape of the curves should be realistic and only the absolute values should be altered by T_i. The velocity distributions obtained in this manner, using the electron temperature, anticipated from the following section, are shown in Figs. 9 and 10. A first estimation whether the velocities determined in this manner are realistic or not can be done by comparing the mass flow through a cross section of

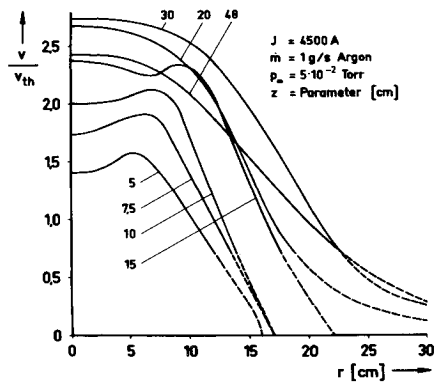

Fig. 8 Radial distributions of the ratio V/V_{th}; $I = 4500$ amp; $\dot{m} = 1$ g/sec.

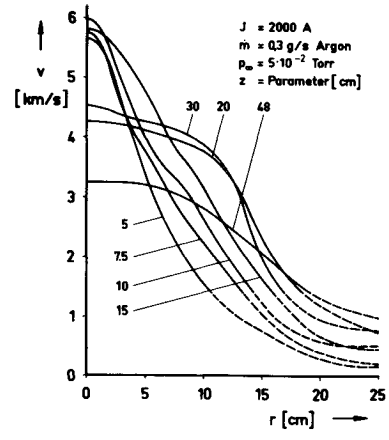

Fig. 9 Radial distributions of the (ion) velocities; $I = 2000$ amp; $\dot{m} = 0.3$ g/sec.

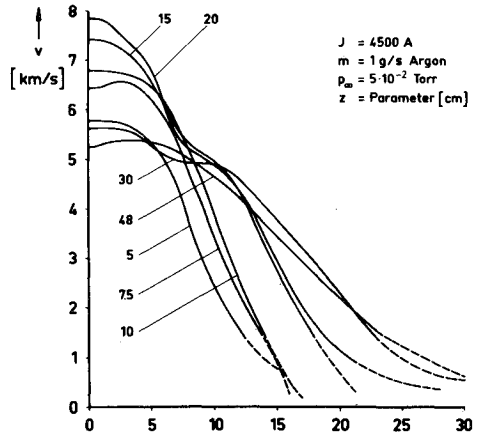

Fig. 10 Radial distributions of the (ion) velocities; $I = 4500$ amp; $\dot{m} = 1$ g/sec.

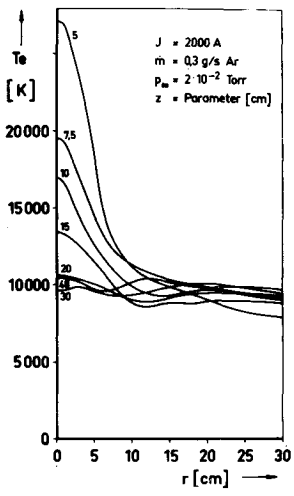

Fig. 11 Radial distributions of the electron temperatures; $I = 2000$ amp; $\dot{m} = 0.3$ g/sec.

the jet with the applied mass flow rate. The plasma therefore is assumed to be fully ionized; hence the density ρ may be expressed by

$$\rho = \Sigma n \cdot m \approx n_i m_i$$

The total mass flow through a cross section of the jet can be calculated from

$$\dot{m} = 2\pi \int_0^{ra} \rho v r \, dr \approx 2\pi m_i \int_0^{ra} n_i v_i r \, dr$$

Using the ion density distributions as outlined in the next section and evaluating the integral, the following behavior of the $\dot{m}$ values may be observed.

With the low current operating conditions ($I = 2000$ amp and 2400 amp), the calculated mass flow through a cross section of the jet at a distance $z = 15$ cm from the nozzle end is within 30% below the applied mass flow rate. At high currents (3500 amp and 4500 amp), the calculated mass flow is within 25% above the applied mass flow rate. This behavior may be explained as follows: with the low currents and regarding the electron temperature distributions, the assumption of full ionization is not completely valid. With the high currents, a part of the ions surely will be double ionized. Therefore the ion density calculated from the ion saturation current and hence also the mass flow through the cross section will be determined too high.

We know that these considerations concerning the mass flow through a cross section are rough ones, but the relative good agreement with the applied mass flow rate shows that the measured values of electron temperature, ion velocity, and ion density are in a realistic order of magnitude.

Electron Temperatures and Ion Densities

From all quantities determinable with Langmuir probes, the electron temperature is the most reliable, even with flowing plasmas. The probes in this case should be cylindrical ones with a large ratio of length to diameter and the main axis should be aligned with the flow direction. Involving the theoretical considerations of Laframboise, Sonin et al.[15,16] the electron temperature is determinable from the semilogarithmic plot of the electron current vs the probe voltage.

The evaluation was done with the same plot of the probe current as used in order to determine $I_\perp/I_\parallel$. After subtracting the ion saturation current, the probe current was recorded using a logarithmic amplifier. With the aid of the already mapped streamlines of the ions, the horizontal probe (Fig. 2) was aligned with the flow direction at the point where the characteristic was recorded.

The radial distributions of the electron temperature at the same operating parameters as applied in Figs. 4, 5, 7, and 8 are shown in Figs. 11 and 12. The temperatures in the axis of the jet and near the nozzle exit are subjected to errors of about 30% because the semilogarithmic plot generally yields no straight line. The curvature may be caused by the following mechanisms.

1) The energy distribution of the electrons is not a Maxwellian one in regions near the axis of the jet and near the nozzle exit.

2) Large axial temperature gradients along the length of the probe are existing especially near the nozzle exit.

3) The probe wires are heated too much by large heat fluxes and in consequence of this considerable electron emission arises.

4) The plasma conditions near the axis of the jet are such that the probes are in a transition regime from collision free to collision dominated operation.

Although further investigations are necessary to study the influence of these effects and are planned to be done, we can predict that such a transition regime plays a role. The calculations of Rp/λ_D (Rp-probe radius, λ_D Debye length) yield for the earlier mentioned test conditions values of Rp/λ_D in the range from 63 to 230 ($63 < Rp/\lambda_D < 230$), thus indicating that the probes are operated in the collision-free regime. Kirchhoff, Peterson, and Talbot,[17] however, also investigated the influence of the Knudsen number K; i.e., the ratio of probe radius to the relevant mean free path ($K_i = \lambda ii/Rp$; $K_e = \lambda ee/Rp$, λii = ion-ion free path, λee = electron-electron free path). They found pronounced rounding of the semilogarithmic plot of the electron current in

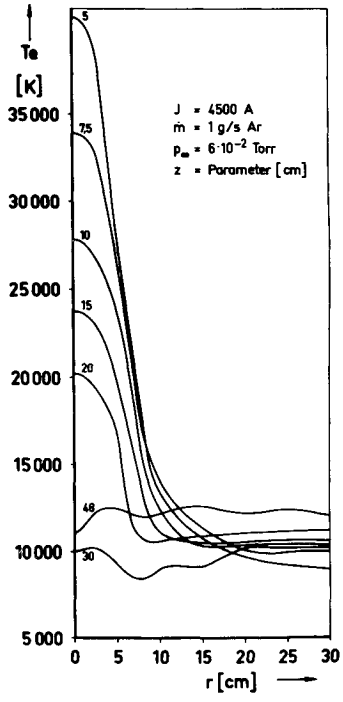

Fig. 12 Radial distributions of the electron temperatures; $I = 4500$ amp; $\dot{m} = 1$ g/sec.

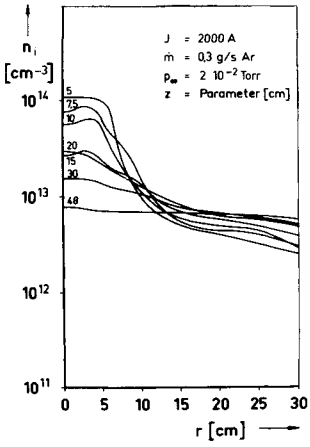

Fig. 13 Ion density profiles; $I = 2000$ amp; $\dot{m} = 0.3$ g/sec.

the retarding-field regime at small values of K_e. The curvature seemed to be the same as observed when evaluating our characteristics. The now calculated ranges of $0.4 < \lambda ii/Rp < 3.3$ and $3.5 < \lambda ee/Rp < 24$ showed that the lower limits of the ratios (corresponding to the region of the jet near the axis and the nozzle) are in the same order of magnitude as those for which Kirchhoff et al. observed and calculated the deviation from free-molecule theory and which are significant for the transition regime. As a further sign of the validity of these considerations we observed an increase of the floating potential up to unexplainable values in the same regions of the jet. This increase with decreasing values of K_i and K_e is observed by these authors[17] too.

Because we recorded the current-voltage characteristics of both probes, (aligned and perpendicular to the flow direction) we determined two electron temperatures, $T_{e\parallel}$ and $T_{e\perp}$ in order to investigate the influence of the ion flow. At larger distances from the nozzle exit $T_{e\perp}$ generally was found to be larger than $T_{e\parallel}$, whereas in neighborhood of the nozzle $T_{e\parallel}$ seems to be larger. This behavior was observed at all operating conditions. The percentage of the maximum error however, $(T_{e\perp}/T_{e\parallel} - 1)$, was in the range of $\pm 10\%$. Furthermore the experiment showed an increase of the error with an increase of the distance z and a decrease with increasing radial distance r. From these observations it can be concluded that the influence of the angle of attack on the determination of the electron temperature is not very severe. This may be because the ion saturation current was subtracted from the total current before performing the semilogarithmic plot.

Generally the maxima of the electron temperature are in the axis of the jet. The absolute values of the maxima increase with the current and decrease with the mass flow rate and the distance from the nozzle end. At a radial distance of about 8 cm all temperature profiles attain a value of about 7000 K–8000 K with "cold" plasmas and of about 10000 K with "hot" plasmas. Note that the mean diameter of the last nozzle segment, acting as the anode, is 12 cm. Whereas from the axis to the point at $r = 8$ cm very steep temperature gradients are predominant, the electron temperature remains nearly constant for larger radial distances. This fact has been observed too while applying microwave techniques for purposes of diagnostics.

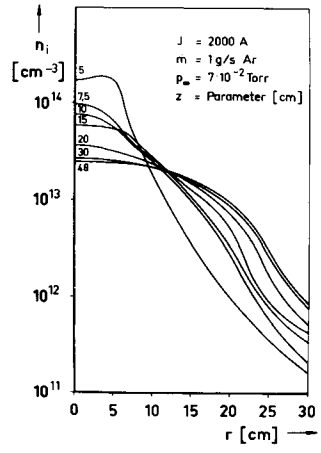

Fig. 14 Ion density profiles; $I = 2000$ amp; $\dot{m} = 1$ g/sec.

From the ion saturation current, measured at ten dimensionless voltage-units below the floating potential, and with the known electron temperature the ion density can be calculated using the theoretical investigations of Laframboise and Sonin.[15,16]

With the main axis of the probe aligned to the flow direction, the ion saturation current can be expressed by the following equation:

$$I_{is} = e n_i A K_i (KT_e/2\pi m_i)^{1/2}$$

where e = electron charge, n_i = ion density, A = probe area, $K_i = f(T_i/T_e, Rp/\lambda_D)$ = current correcting factor, and K = Boltzmann constant.

The dimensionless current correcting factor K_i can be determined from Ref. 15 involving that $63 < Rp/\lambda_D < 230$ and knowing the influence of T_i/T_e to be not very strong (T_i is unknown and assumed to be approximately equal to T_e). The collecting area A of the probe is identified with the geometrical surface. Whereas the electron temperature is not very strongly affected by a disalignment of the main probe axis from the flow direction, the effect on the ion saturation current is much more severe. Therefore much care is necessary to achieve a good alignment. As Kirchhoff et al. pointed out there is an influence of K_i and K_e too in the transition regime on the ion saturation current. Furthermore T_e is subjected to errors near the axis of the jet. Therefore the ion density will be subjected to uncertainties especially in the centerline and in front of the nozzle.

The radial distributions of the ion densities at various distances z from the nozzle are shown in Figs. 13 and 14 for $I = 2000$ amp, $\dot{m} = 0.3$ g/sec, and 1 g/sec, respectively. The behavior at $I = 4500$ amp, $\dot{m} = 1$ g/sec is similar to that at 2000 amp, 0.3 g/sec except that the densities are generally higher by a factor of two. This may be caused by the following two effects.

1) As already mentioned the electron temperatures are in this region of such a magnitude that a considerable fraction of the gas is double ionized. Therefore the ion densities near the nozzle exit definitely will be determined too high.

2) The input power is increased due to a higher current and a higher arc voltage ($I = 2000$ amp, $U_A = 32$ v; $I = 4500$ amp, and $U_A = 48$ v). It can be shown from the complete set of curves, that the latter effect is the predominant one.

As examples we have chosen a higher and a lower mass flow rate at the same current of 2000 amp thus marking a "hot" and a "cold" plasma. With the low mass flow rate we find remarkable density gradients in the radial range of 5–10 cm at lower distances z; in the range from 10 to 30 cm these gradients are considerably smaller. In the case of the higher mass flow rates we have steep density gradients up to large radial distances. The consequence are differences of the ion density between both operating conditions of up to two orders of magnitude at a radial distance of 30 cm. This means a cooling of the plasma at the boundary of the jet, caused by energy transfer to the dense neutral gas surrounding a hot core.

With regard to the operation of plasma accelerators in vacuum facilities at ambient pressures of higher than 10^{-4} torr the question often arises whether neutral gas from outside is sucked into the jet and takes part in the acceleration mechanism. An estimation whether this "entrainment" is present can be obtained by calculating the static pressure in the jet as the sum of the partial pressures of the various species. Considering only the contributions of ions and electrons and assuming $T_i = \frac{1}{3}T_e$ as the lower limit (thus describing an unfavorable case), the static pressure becomes

$$p^* = \Sigma nKT = \frac{4nKT_e}{3} (n_e = n_i)$$

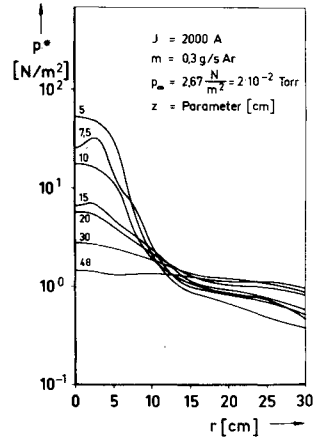

Fig. 15 Profiles of the static pressure. $I = 2000$ **amp;** $\dot{m} = 1$ **g/sec.**

The profiles of this pressure, calculated from the measured distributions of the ion density and the electron temperature, show that at all operating conditions the static pressure in those regions where $\mathbf{j} \times \mathbf{B}$ volume forces are acting is above the ambient pressure. For example Fig. 15 shows the pressure profiles for the operating conditions $I = 2000$ amp, $\dot{m} = 0.3$ g/sec. Suction of gas from outside into that region of the jet where electromagnetic forces are acting therefore can be excluded.

Conclusions

The present investigations are a contribution of understanding this type of MPD accelerator. Furthermore it can be seen that Langmuir probes are a good diagnostic tool to determine quantities like electron temperature, ion density, Mach number, directed ion velocity, and ion flow pattern. The good agreement of the mass flow through a cross section of the jet with the applied mass flow rate shows that the determined radial distributions of T_e, n_i, and V_i are realistic. To complete the series of data of the various quantities in the exhaust plasma as well as to confirm the measurements with electric probes, it is intended to do further diagnostic investigations as follows: 1) The ion temperature and the ion density will be measured using spectroscopic techniques. 2) The directed electron velocity will be determined with the $\mathbf{v} \times \mathbf{B}$ method. 3) Applying Hall probes, the distribution of the discharge current outside of the nozzle will be determined. This is necessary to give information of that part of the $\mathbf{j} \times \mathbf{B}$-forces, acting in the freejet region.

Besides the investigations of the plasma jet, the development of diagnostic techniques with electric and magnetic probes is a further aim of efforts. Therefore the comparison between the ion velocities (determined with Langmuir probes and with spectroscopic means) and the electron velocities ($\mathbf{v} \times \mathbf{B}$ method) is expected to give interesting results concerning the applicability of the various methods.

References

[1] Clark, K. E., Jahn, R. G., and von Jaskowsky, W. F., "Distribution of Momentum and Propellant in a Quasi-Steady MPD Discharge," AIAA Paper 72-497, Bethesda, Md., 1972.

[2] Clark, K. E., "Quasi-Steady Plasma Acceleration," AMS Rept. 851, 1969, Princeton Univ., Princeton, N.J.

[3] Malliaris, A. C. et al., "Quasi-Steady MPD Propulsion at High Power," Final TR AVSD-0146-71-RR, 1971, AVCO Corp., Wilmington, Mass.

[4] Hoell, J. M., Burlock, J., and Jarrett, O., "Velocity and Thrust Measurements in a Quasi-Steady MPD Thruster," *AIAA Journal*, Vol. 9, No. 10, Oct. 1971, pp. 1969–1974.

[5] Michels, C. J. and York, T. M., "Exhaust Flow and Propulsion Characteristics of a Pulsed MPD Arc Thruster," AIAA Paper 72-500, Bethesda, Md., 1972.

[6] Hügel, H., "Untersuchungen am eigenmagnetischen Plasmabeschleuniger," *Raumfahrtforschung*, Heft 5, Sept.–Oct. 1972.

[7] Hügel, H., "Flow Rate Limitations in the Self-Field Accelerator," AIAA Paper 73-1094, Stateline, Nev., 1973.

[8] Jakubowski, A. K., "Effect of Angle of Incidence on the Response of Cylindrical Electrostatic Probes at Supersonic Speeds," *AIAA Journal*, Vol. 10, No. 8, Aug. 1972, p. 988.

[9] Sonin, A. A., "Free-Molecule Langmuir Probe and It's Use in Flowfield Studies," *AIAA Journal*, Vol. 4, No. 9, Sept. 1966, p. 1588.

[10] Maisenhälder, F. and Mayerhofer, W., "On an Angular Effect of Cylindrical Langmuir Probes in Flowing Plasmas," Paper 5.1.2.6 presented at the XIth International Conference on Phenomena in Ionized Gases, Prague, Czechoslovakia, Sept. 1973.

[11] Maisenhälder, F. and Schock, W., "Verteilung von Geschwindigkeiten und Strömen in MPD-Strahlen," *Zeitschrift für angewandte Physik*, 30 Bd., 4. Heft, 1970, S. 295–299.

[12] Kanal, M., "Theory of Current Collection of Moving Cylindrical Probes," *Journal of Applied Physics*, Vol. 35, No. 6, June 1964, pp. 1097–1703.

[13] Johnson, B. H., Murphree, D. L., "Plasma Velocity Determination by Electrostatic Probes," *AIAA Journal*, Vol. 7, No. 10, Oct. 1969, p. 2028.

[14] Beth, M.-U., private communication, Nov. 1972.

[15] Laframboise, J. G., UTIAS-Rept. 100, June 1966, Univ. of Toronto Institute of Aerospace Sciences, Toronto, Ontario, Canada.

[16] Sonin, A. A., UTIAS-Rept. 109, Aug. 1965, Univ. of Toronto Institute of Aerospace Sciences, Toronto, Ontario, Canada.

[17] Kirchhoff, R. H., Peterson, W. E., and Talbot, L., "An Experimental Study of the Cylindrical Langmuir Probe Response in the Transition Regime," *AIAA Journal*, Vol. 9, No. 9, Sept. 1971, p. 1680.